Acta Crystallographica Section F
Structural Biology and Crystallization Communications
ISSN 1744-3091

Sita R. Meena, Shanti P. Gangwar and Ajay K. Saxena*

Structural Biology Laboratory, School of Life Sciences, Jawaharlal Nehru University, New Delhi 110 067, USA

Correspondence e-mail: ajaysaxena@mail.jnu.ac.in

Received 22 February 2012
Accepted 30 March 2012

Purification, crystallization and preliminary X-ray crystallographic analysis of the ATPase domain of human TAP in nucleotide-free and ADP-, vanadate- and azide-complexed forms

The human transporter associated with antigen processing (TAP) protein belongs to the ATP-binding cassette (ABC) transporter superfamily and is formed by the heterodimerization of TAP1 and TAP2 subunits. TAP selectively pumps cytosolic peptides into the lumen of the endoplasmic reticulum in an ATP-dependent manner. The catalytic cycle of the ATPase domain of TAP is not understood at the molecular level. The structures of catalytic intermediates of the ATPase domain of TAP will contribute to the understanding of the chemical mechanism of ATP hydrolysis. In order to understand this mechanism, the ATPase domain of human TAP1 (NBD1) was expressed and purified, crystallized in nucleotide-free and transition-state complex forms and X-ray crystallographic studies were performed. The NBD1 protein was crystallized (i) in the nucleotide-free apo form; (ii) in complex with ADP–Mg^{2+}, mimicking the product-bound state; (iii) in complex with vanadate–ADP–Mg^{2+}, mimicking the ATP-bound state; and (iv) in complex with azide–ADP–Mg^{2+}, also mimicking the ATP-bound state. X-ray diffraction data sets were collected for apo and complexed NBD1 using an in-house X-ray diffraction facility at a wavelength of 1.5418 Å. The apo and complexed NBD1 crystals belonged to the primitive hexagonal space group $P6_2$, with one monomer in the asymmetric unit. Here, the crystallization, data collection and preliminary crystallographic analysis of apo and complexed NBD1 are reported.

1. Introduction

The human transporter associated with antigen processing (TAP) is a heterodimer composed of TAP1 and TAP2 subunits and is found in the ER membranes of all nucleated cell organisms with an adaptive immune system (Lankat-Buttgereit & Tampé, 2002). TAP translocates peptides derived from the proteosomal degradation of proteins from the cytosol into the endoplasmic reticulum, where they bind nascent MHC class I molecules (Koch & Tampé, 2006; Wearsch & Cresswell, 2008). Each TAP subunit consists of an N-terminal membrane-spanning domain and a C-terminal nucleotide-binding domain (NBD) (Kelly *et al.*, 1992). ATP is an essential requirement for antigen translocation by TAP and other ABC transporters. The binding and chemical energy of ATP hydrolysis by TAP are used in different stages of the transport cycle.

The TAP NBD contains all of the residues that are required to form a complete ATP-binding site. Two ATP-binding sites are formed in each TAP when TAP1 NBD and TAP2 NBD form a head-to-tail dimer; residues from each monomer contribute to the binding site (Jones & George, 1999). The consensus residues of TAP1 NBD and TAP2 NBD differ significantly from each other, but appear to bind ATP and ADP with similar affinities. ATP-hydrolysis transition states can be trapped in both TAP1 and TAP2 NBD (Chen *et al.*, 2003; Lapinski *et al.*, 2003). The significance of the asymmetry in the TAP NBDs is not clear. The crystal structure of the TAP1–TAP2 NBD complex is not available and this may be because of a relatively weak interaction at a degenerate site (Procko *et al.*, 2006). Structures of an artificial TAP1–TAP1 NBD homodimeric structure and of TAP1

NBD in complex with ADP and Mg^{2+} have been determined (Procko *et al.*, 2006; Gaudet & Wiley, 2001).

No consensus has been derived regarding the mechanism of ATP hydrolysis by TAP despite the wealth of structural and biochemical data that are available. Several major models have been proposed regarding the mechanism of ATP hydrolysis by TAP NBDs (Abele & Tampé, 2004; Higgins & Linton, 2004; Senior & Gadsby, 1997; Jones *et al.*, 2009). High-resolution structures of the catalytic intermediates of TAP NBD domains will contribute significantly towards understanding the chemical mechanism of ATP hydrolysis.

Here, we report the cloning, purification, crystallization and preliminary X-ray crystallographic studies of NBD1 (i) in the nucleotide-free apo form; (ii) in complex with ADP–Mg^{2+}, which mimics the product-bound state; (iii) in complex with vanadate–ADP–Mg^{2+}, which mimics the ATP-bound form; and (iv) in complex with azide–ADP–Mg^{2+}, which also mimics the ATP-bound form.

2. Materials and methods

2.1. Expression and purification of NBD1

The gene encoding residues 500–748 of human TAP1 (NBD1) was obtained by polymerase chain reaction using full-length human TAP1 cDNA clone (obtained from Dr D. N. Garboczi, NIH). The primers 5′-A TTC CAT ATG GAG GGC CTT GTC CAG TTC-3′ and 3′-A CGC GTC GAC TTA TCA TTC TGG AGC ATC TGC AGG-5′ were used in NBD1 gene amplification. The NBD1 gene was cloned in pET28a(+) vector containing an N-terminal 6×His tag and thrombin cleavage site.

The NBD1 plasmid was transformed into *Escherichia coli* BL21 (DE3) cells. The cells were grown in Luria–Bertani medium containing 25 µg ml^{-1} kanamycin at 310 K until the OD_{600} reached 0.5–0.6. The culture was induced with 1 m*M* isopropyl *β*-D-1-thiogalactopyranoside at 310 K and was grown for a further 4 h. NBD1 was expressed as inclusion bodies in *E. coli*. We optimized the fermentation conditions to obtain expression of NBD1 in the soluble cell fraction. According to the optimized protocol, the culture was grown at 310 K until the OD_{600} reached 0.5–0.6. The culture was induced with 6 µ*M* isopropyl *β*-D-1-thiogalactopyranoside and grown for a further 12 h at 289 K. The cells were harvested by centrifugation at 10 000*g* for 15 min at 277 K, washed with 20 m*M* Tris–HCl pH 8.0 and pelleted again by centrifugation. The pellet was suspended in lysis buffer consisting of 25 m*M* Tris–HCl pH 8.0, 150 m*M* NaCl, 1 m*M* phenylmethylsulfonyl fluoride (PMSF), 1 m*M* benzamidine–HCl, 3 m*M* *β*-mercaptoethanol (*β*-ME), 10 m*M* imidazole, 10% glycerol, 5 m*M* $MgCl_2$, 0.1% Triton X-100, 0.15 mg ml^{-1} lysozyme and kept on ice for 1 h. The cells were lysed by sonication, centrifuged at 12 000*g* for 15 min and the supernatant was collected.

For Ni–NTA chromatography, the supernatant was mixed with pre-equilibration buffer consisting of 25 m*M* Tris–HCl pH 8.0, 150 m*M* NaCl, 1 m*M* PMSF, 1 m*M* benzamidine–HCl, 3 m*M* *β*-ME, 10% glycerol, 0.1% Triton X-100, 5 m*M* $MgCl_2$, 20 m*M* imidazole. The protein mixture was incubated with Ni–NTA resin by shaking for 2 h at 277 K on a 360° rocker. The protein was loaded into an empty column and washed with buffer consisting of 25 m*M* Tris–HCl pH 8.0, 300 m*M* NaCl, 1 m*M* PMSF, 1 m*M* benzamidine–HCl, 3 m*M* *β*-ME, 10% glycerol, 5 m*M* $MgCl_2$, 30 m*M* imidazole. After washing, the protein was eluted using 25 m*M* Tris–HCl pH 8.0, 150 m*M* NaCl, 0.5 m*M* PMSF, 0.5 m*M* benzamidine–HCl, 3 m*M* *β*-ME, 10% glycerol, 5 m*M* $MgCl_2$, 300 m*M* imidazole. The purified NBD1 fractions were pooled and concentrated using Amicon-10 Ultra (Millipore). The concentrated protein was loaded onto a Sephacryl 200 HR size-exclusion column pre-equilibrated with buffer consisting of 20 m*M* Tris–HCl pH 8.0, 150 m*M* NaCl, 0.5 m*M* PMSF, 0.5 m*M* benzamidine–HCl, 3 m*M* *β*-ME, 10% glycerol, 5 m*M* $MgCl_2$. The NBD1 eluted as a monomer from the size-exclusion column and had a purity greater than 98% according to mass spectrometry and SDS–PAGE analysis (Fig. 1). The purified NBD1 contained a total of 269 residues: 21 residues from the vector, including a 6×His tag and a thrombin-cleavage site, and residues 500–748 of human TAP1.

2.2. Crystallization

The purified NBD1 was concentrated to 30 mg ml^{-1} in buffer consisting of 20 m*M* Tris–HCl pH 8.0, 150 m*M* NaCl, 3 m*M* *β*-ME, 10% glycerol, 5 m*M* $MgCl_2$. Initial crystallization conditions were

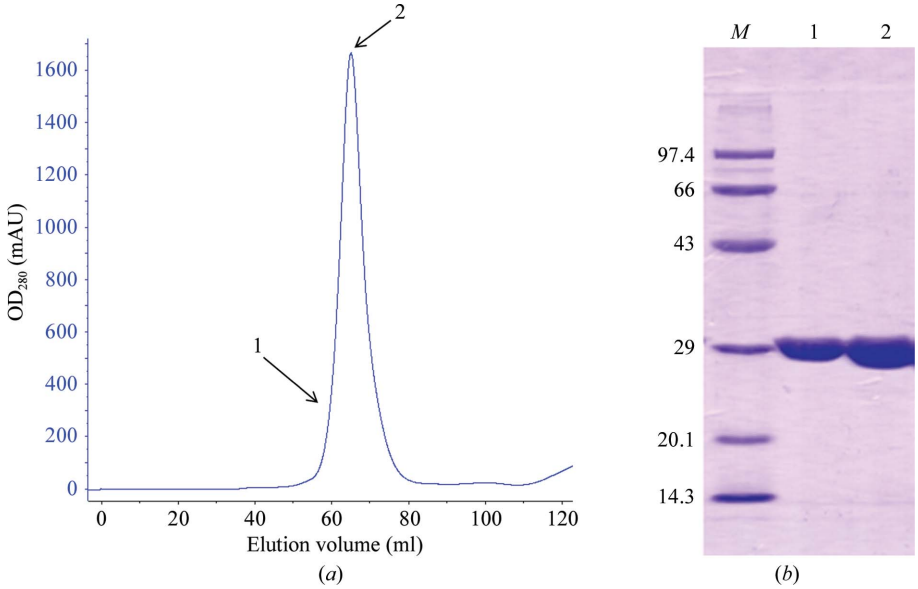

Figure 1
(*a*) Elution profile of the purification of NBD1 using a Sephacryl 200 (16/60) HR column. The major peak corresponds to NBD1. (*b*) SDS–PAGE analysis after size-exclusion chromatography of purified NBD1. Lane *M*, molecular-weight markers (kDa); lanes 1 and 2, SDS–PAGE analysis of eluted fractions containing purified NBD1.

identified using Crystal Screen, Crystal Screen 2 and PEG/Ion from Hampton Research. All crystallization experiments were performed at 277 K using the hanging-drop vapour-diffusion technique.

2.2.1. Nucleotide-free apo NBD1. 1 µl apo NBD1 (at a concentration of ∼30 mg ml^{-1}) was mixed with 1 µl reservoir solution and equilibrated against 500 µl reservoir solution consisting of 25%(*w*/*v*) PEG 4000, 100 m*M* Tris–HCl pH 8.0, 200 m*M* $MgCl_2$. Crystals appeared in 15–40%(*w*/*v*) PEG 4000 and the pH range 6.5–9.0. The best crystals were obtained using a reservoir solution consisting of 25%(*w*/*v*) PEG 4000, 100 m*M* Tris–HCl pH 8.0, 200 m*M* $MgCl_2$. The rhombohedral-shaped apo NBD1 crystals appeared within 3–4 d and had typical dimensions of 0.6 × 0.5 × 0.2 mm (Fig. 2*a*).

2.2.2. NBD1 complex with ADP–Mg^{2+}. The NBD1–ADP–Mg^{2+} complex crystals were obtained by mixing 1 µl protein solution containing NBD1 at ∼15 mg ml^{-1} and 5 m*M* ADP with 1 µl reservoir solution consisting of 25%(*w*/*v*) PEG 4000, 100 m*M* Tris–HCl pH 8.0, 200 m*M* $MgCl_2$. The crystals appeared after 7 d and grew in a rhombohedral shape with typical dimensions of 0.6 × 0.4 × 0.2 mm (Fig. 2*b*).

2.2.3. NBD1 complex with ADP–Mg^{2+}–vanadate. The NBD1–ADP–Mg^{2+}–vanadate complex crystals were obtained by mixing 1 µl protein solution containing NBD1 at ∼30 mg ml^{-1}, 10 m*M* sodium orthovanadate and 5 m*M* ADP with 1 µl reservoir solution consisting of 25%(*w*/*v*) PEG 4000, 100 m*M* Tris–HCl pH 8.0, 200 m*M* $MgCl_2$. The vanadate solution was prepared by boiling in water for 5 min and cooling to room temperature and was mixed with the reservoir solution. The complex crystals appeared after 7 d and grew in a rhombohedral shape with typical dimensions of 0.3 × 0.3 × 0.1 mm (Fig. 2*c*).

2.2.4. NBD1 complex with ADP–Mg^{2+}–azide. The NBD1–ADP–Mg^{2+}–azide complex crystals were obtained by mixing 1 µl protein solution containing NBD1 at ∼30 mg ml^{-1}, 10 m*M* NaN_3 and 5 m*M* ADP with 1 µl reservoir solution consisting of 25%(*w*/*v*) PEG 4000, 100 m*M* Tris–HCl pH 8.0, 200 m*M* $MgCl_2$. The complex crystals appeared after 10 d and grew in a rhombohedral shape with typical dimensions of 0.4 × 0.2 × 0.1 mm (Fig. 2*d*).

2.3. Intensity data collection and processing

For intensity data collection, single crystals were transferred into a solution consisting of 30%(*w*/*v*) PEG 4000, 100 m*M* Tris–HCl pH 8.0, 200 m*M* $MgCl_2$ and cooled directly in a liquid-nitrogen stream. The 30%(*w*/*v*) PEG 4000 acts as a good cryoprotectant for diffraction experiments at cryogenic temperature.

X-ray diffraction data were collected at 100 K using a MAR 300 image-plate scanner mounted on a Bruker X-ray generator at the Advanced Instrument Research Facility (AIRF), Jawaharlal Nehru University, New Delhi. The intensity data-collection ranges for each NBD1 data set are given in Table 1. Indexing and integration of the images were performed with *MOSFLM* (Leslie, 1992) and scaling and merging of the data sets were performed with *SCALA* (Winn *et al.*, 2011). F_{obs} values were obtained using the *TRUNCATE* program from the *CCP*4 suite (Winn *et al.*, 2011).

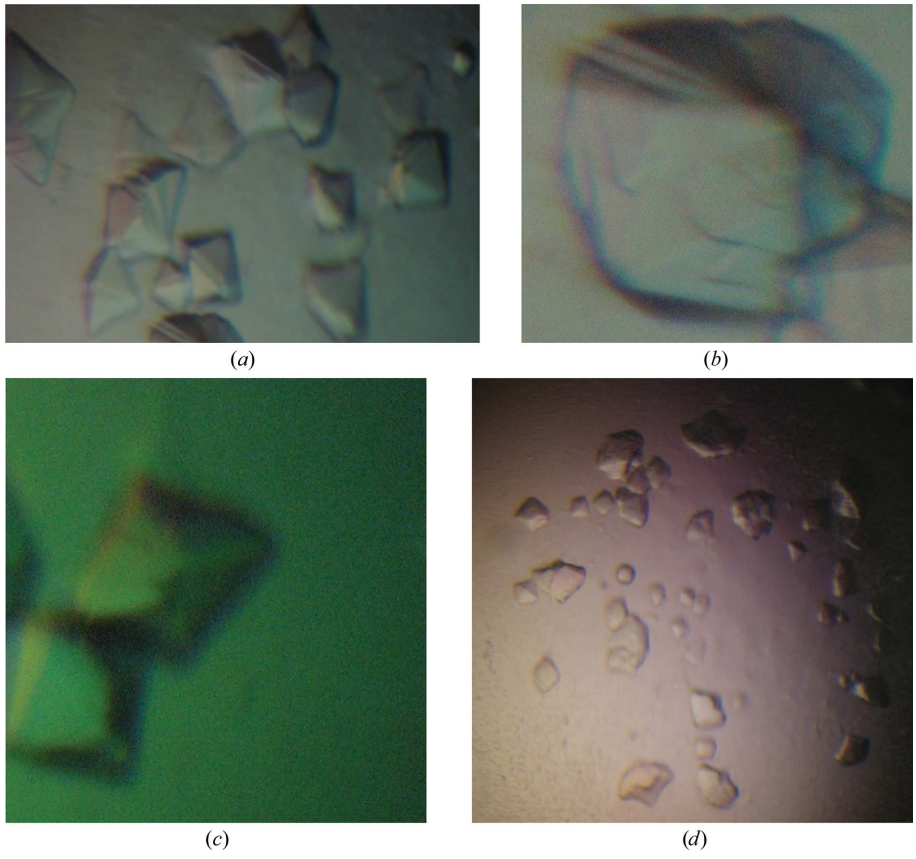

Figure 2
Single crystals of NBD1 (*a*) in the nucleotide-free apo form, (*b*) in the ADP–Mg^{2+}-complexed form, (*c*) in the ADP–Mg^{2+}–vanadate-complexed form and (*d*) in the ADP–Mg^{2+}–azide-complexed form. The equipment used to obtain the image could not be accurately calibrated to capture true images. The crystals were grown using the hanging-drop vapour-diffusion technique at 277 K.

Table 1
Intensity data-collection and processing statistics..

Values in parentheses are for the last resolution shell.

Data set	Nucleotide-free	ADP–Mg^{2+}	ADP–Mg^{2+}–vanadate	ADP–Mg^{2+}–azide
Resolution (Å)	27.8–2.9 (3.11–2.95)	29.7–2.8 (2.97–2.82)	28.1–2.9 (3.06–2.90)	27.7–2.9 (3.11–2.95)
Wavelength (Å)	1.5418	1.5418	1.5418	1.5418
X-ray source	Bruker	Bruker	Bruker	Bruker
Rotation range (°)	155	91	140	180
Space group	$P6_2$	$P6_2$	$P6_2$	$P6_2$
Unit-cell parameters (Å)	$a = b = 84.9$, $c = 83.2$	$a = b = 84.8$, $c = 83.3$	$a = b = 85.9$, $c = 82.7$	$a = b = 84.5$, $c = 82.9$
Total reflections	59877	43813	57952	70812
Unique reflections	7277	7584	7760	7159
Completeness (%)	99.9 (100)	91.5 (93.5)	99.8 (99.7)	99.9 (100)
R_{merge}† (%)	13.2 (50.1)	12.2 (55.8)	12.1 (55.0)	16.1 (66.8)
Average $I/\sigma(I)$	13.9 (3.9)	11.1 (2.9)	13.5 (3.4)	14.3 (3.2)
Multiplicity	8.2	5.8	7.5	9.9

† $R_{merge} = \sum_{hkl}\sum_i |I_i(hkl) - \langle I(hkl)\rangle| / \sum_{hkl}\sum_i I_i(hkl)$, where $I_i(hkl)$ is the ith intensity measurement of reflection hkl and $\langle I(hkl)\rangle$ is the average intensity of this reflection.

3. Results and discussion

The apo and complexed NBD1 crystals belonged to space group $P6_2$ with one monomer in the asymmetric unit. All of the crystals diffracted to resolutions in the range 2.8–3.0 Å. Details of the intensity data-collection and processing statistics are given in Table 1. Complete and high-quality diffraction data were collected for the apo and complexed NBD1 crystals.

3.1. Nucleotide-free apo NBD1

The apo NBD1 crystals were grown without nucleotide and diffracted to 2.9 Å resolution. The crystallization condition for the apo NBD1 crystals differed from those previously reported for TAP1 NBD crystals (Gaudet & Wiley, 2001; Procko *et al.*, 2006). The apo NBD1 crystals were grown at a higher pH with a higher $MgCl_2$ concentration and with PEG 4000 as precipitant. However, the crystals belonged to space group $P6_2$, as in the case of the TAP1 NBD structure (Gaudet & Wiley, 2001), but with different unit-cell parameters. With one molecule of apo NBD1 in the asymmetric unit, the Matthews coefficient V_M was 2.98 $Å^3\ Da^{-1}$, which corresponds to a solvent content of 58.73% (Matthews, 1968).

3.2. NBD1 complex with ADP–Mg^{2+}

The crystals were grown in the presence of Mg^{2+} and 10 m*M* ADP. The rectangular bipyramid-shaped crystals appeared at 277 K. The crystals diffracted to 2.8 Å resolution and belonged to space group $P6_2$. The unit-cell parameters of the current complex were similar to those of the apo NBD1 crystal, but differed from those of the TAP1 NBD structure (Gaudet & Wiley, 2001; Procko *et al.*, 2006). With one NBD1 complex in the asymmetric unit, the Matthews coefficient V_M was 2.97 $Å^3\ Da^{-1}$, which corresponds to a solvent content of 58.68% (Matthews, 1968).

3.3. NBD1 complex with ADP–Mg^{2+}–vanadate

The crystals were grown in the presence of ADP, Mg^{2+} and vanadate. The rectangular bipyramid-shaped crystals appeared at 277 K. A single crystal was harvested in a 0.2 mm nylon loop and was flash-cooled in a liquid-nitrogen stream. Diffraction data were collected using a MAR 300 imaging-plate scanner mounted on a Bruker X-ray generator. The crystal diffracted to a maximum resolution of 2.9 Å. With one NBD1 complex in the asymmetric unit, the Matthews coefficient V_M was 2.93 $Å^3\ Da^{-1}$, which corresponds to a solvent content of 58.06% (Matthews, 1968).

3.4. NBD1 complex with ADP–Mg^{2+}–azide

The crystals were grown in the presence of ADP, Mg^{2+} and azide. Diffraction data were collected using a MAR 300 imaging-plate scanner mounted on a Bruker X-ray generator. These crystals diffracted X-rays to a maximum resolution of 2.9 Å and belonged to space group $P6_2$. With one NBD1 complex in the asymmetric unit, the Matthews coefficient was 2.94 $Å^3\ Da^{-1}$, which corresponds to a solvent content of 58.19% (Matthews, 1968).

To obtain phase information, molecular-replacement analysis was performed using *Phaser* from the *CCP*4 suite (Winn *et al.*, 2011). The TAP1 NBD structure (PDB entry 1jj7; Gaudet & Wiley, 2001) was used as an input model for phase analysis. Molecular-replacement analysis yielded useful phases for the apo and complexed NBD1 structures. Structure determinations of apo and complexed NBD1 are currently in progress.

AKS was supported by a CSIR grant for this work. Grants from UGC Networking, JNU Capacity Buildup and the DST Purse are gratefully acknowledged. SRM is supported by a Senior Research Fellowship from DBT, India. SPG is supported by a Junior Research Fellowship from UGC, India. We acknowledge the crystallization and X-ray diffraction facility of the Advanced Instrumentation Research Facility (AIRF), Jawaharlal Nehru University for allowing us to conduct the X-ray diffraction experiments.

References

Abele, R. & Tampé, R. (2004). *Physiology*, **19**, 216–224.
Chen, M., Abele, R. & Tampé, R. (2003). *J. Biol. Chem.* **278**, 29686–29692.
Gaudet, R. & Wiley, D. C. (2001). *EMBO J.* **20**, 4964–4972.
Higgins, C. F. & Linton, K. J. (2004). *Nature Struct. Mol. Biol.* **11**, 918–926.
Jones, P. M. & George, A. M. (1999). *FEMS Microbiol. Lett.* **179**, 187–202.
Jones, P. M., O'Mara, M. L. & George, A. M. (2009). *Trends Biochem. Sci.* **34**, 520–531.
Kelly, A., Powis, S. H., Kerr, L. A., Mockridge, I., Elliott, T., Bastin, J., Uchanska-Ziegler, B., Ziegler, A., Trowsdale, J. & Townsend, A. (1992). *Nature (London)*, **355**, 641–644.
Koch, J. & Tampé, R. (2006). *Cell. Mol. Life Sci.* **63**, 653–662.
Lankat-Buttgereit, B. & Tampé, R. (2002). *Physiol. Rev.* **82**, 187–204.
Lapinski, P. E., Raghuraman, G. & Raghavan, M. (2003). *J. Biol. Chem.* **278**, 8229–8237.
Leslie, A. G. W. (1992). *Jnt CCP4/ESF–EACBM Newsl. Protein Crystallogr.* **26**.
Matthews, B. W. (1968). *J. Mol. Biol.* **33**, 491–497.
Procko, E., Ferrin-O'Connell, I., Ng, S. L. & Gaudet, R. (2006). *Mol. Cell*, **24**, 51–62.
Senior, A. E. & Gadsby, D. C. (1997). *Semin. Cancer Biol.* **8**, 143–150.
Wearsch, P. A. & Cresswell, P. (2008). *Curr. Opin. Cell Biol.* **20**, 624–631.
Winn, M. D. *et al.* (2011). *Acta Cryst.* D**67**, 235–242.